

Carboniferous integrative stratigraphy and timescale of China

Xiangdong WANG^{1,2*}, Keyi HU^{2†}, Wenkun QIE¹, Qingyi SHENG³, Bo CHEN⁴, Wei LIN¹,
Le YAO³, Qiulai WANG¹, Yuping QI¹, Jitao CHEN¹, Zhuoting LIAO³ & Junjun SONG³

¹ CAS Key Laboratory of Economic Stratigraphy and Palaeogeography, Nanjing Institute of Geology and Palaeontology, Chinese Academy of Sciences, Nanjing 210008, China;

² Center for Research and Education on Biological Evolution and Environment, Nanjing University, Nanjing 210023, China;

³ Nanjing Institute of Geology and Palaeontology, Chinese Academy of Sciences, Nanjing 210008, China;

⁴ State Key Laboratory of Palaeobiology and Stratigraphy, Nanjing Institute of Geology and Palaeontology, Chinese Academy of Sciences, Nanjing 210008, China

Received September 21, 2017; revised July 2, 2018; accepted July 20, 2018; published online September 4, 2018

Abstract The Carboniferous period lasted about 60 Myr, from ~358.9 Ma to ~298.9 Ma. According to the International Commission on Stratigraphy, the Carboniferous System is subdivided into two subsystems, i.e., Mississippian and Pennsylvanian, including 6 series and 7 stages. The Global Stratotype Sections and Points (GSSPs) of three stages have been ratified, the Tournaisian, Viséan, and Bashkirian stages. The GSSPs of the remaining four stages (i.e., the Serpukhovian, Moscovian, Kasimovian, and Gzhelian) have not been ratified so far. This paper outlines Carboniferous stratigraphic subdivision and correlation on the basis of detailed biostratigraphy mainly from South China, and summarizes the Carboniferous chronostratigraphic framework of China. High-resolution biostratigraphic study reveals 37 conodont zones, 24 foraminiferal (including fusulinid) zones, 13 ammonoid zones, 10 brachiopod zones, and 10 rugose coral zones in the Carboniferous of China. The biostratigraphic framework based on these biozones warrants the precise correlation of regional stratigraphy of China (including 2 subsystems, 4 series, and 8 stages) to that of the other regions globally. Meanwhile, the Carboniferous chemo-, sequence-, cyclo-, and event-stratigraphy of China have been intensively studied and can also be correlated worldwide. Future studies on the Carboniferous in China should focus on (1) the correlation between shallow- and deep-water facies and between marine and continental facies, (2) high-resolution astronomical cyclostratigraphy, and (3) paleoenvironment and paleoclimate analysis based on geochemical proxies such as strontium and oxygen isotopes, as well as stomatal indices of fossil plants.

Keywords Carboniferous, Chronostratigraphy, Biostratigraphy, Chemostratigraphy, Event stratigraphy, Stratotype, Stratigraphic correlation

Citation: Wang X D, Hu K Y, Qie W K, Sheng Q Y, Chen B, Lin W, Yao L, Wang Q L, Qi Y P, Chen J T, Liao Z T, Song J J. 2019. Carboniferous integrative stratigraphy and timescale of China. *Science China Earth Sciences*, 62: 135–153, <https://doi.org/10.1007/s11430-017-9253-7>

1. Introduction

The Carboniferous (358.9–298.9 Ma) is the main period of coal formation in Earth history. It is one of the main target strata of fossil energy that presently yield coal in middle and east Europe. Rocks of this age hosted the earliest oilfield in

US history, and shale gas is being exploited in the central US today. An international collaborative organization for Carboniferous research was established as early as in 1927 when the first Carboniferous Congress was held in Heerlen, the Netherlands. Since then, totally 18 congresses have been regularly held around the world, which greatly promotes regional and global correlation of the Carboniferous, and establishment of subdivision standard.

* Corresponding authors (email: xdwang@nigpas.ac.cn)

† Corresponding authors (email: kyhu@nju.edu.cn)

The Carboniferous is a period of intense global tectonics. The Hercynian Orogeny, which started in the early Carboniferous, resulted from collision between the Euramerica and Gondwana continents, forming the Variscan-Ouachita-Alleghanian (VOA) orogenic belt. The orogenic uplift likely enhanced continental weathering and increased organic carbon burial (Saltzman et al., 2000). Expansion of land plants at this time might also have increased organic carbon burial (Popp et al., 1986; Berner, 1990, 1997; Mii et al., 1999). These two events collectively resulted in the Carboniferous glaciation (Chen et al., 2018), one of the major icehouses of the Phanerozoic. Waxing and waning of glaciation caused frequent glacio-eustatic changes, which resulted in common occurrence of stratigraphic discontinuities, especially in Euramerica due to the superimposed orogenic uplift.

The Carboniferous is a period of rapid evolution of marine invertebrates, including conodonts, foraminifera, ammonoids, rugose corals, brachiopods, bryozoans, echinoderms, and radiolaria, among which foraminifera and conodont are the main index fossils for subdivision and correlation of shallow- and deep-water successions, respectively. During the Mississippian, the oceans were well interconnected, and the endemism of marine invertebrates was not so distinct, whereas in the Pennsylvanian, endemism became more obvious (Walliser, 1995) due to closure of the Rheic Ocean (Montañez and Poulsen, 2013). Amphibians evolved rapidly during the Carboniferous; certain types had been free from water and evolved into early amniotes. Giant dragonflies with a wingspan of close to 1 m also occurred at this time. Land plants flourished during the Carboniferous. Mississippian plants are similar to those of the late Devonian, dominated by primitive ferns, whereas true ferns and seed ferns existed in the Pennsylvanian. Gymnosperm has also arisen at this time. With expansion of land area, land plants invaded continental settings from coastal regions, forming large-scale forests and swamps, which provided prerequisite conditions for coal formation.

In a very general sense, the Carboniferous can be clearly subdivided into two deposits with respect to facies. The older deposits, dominated by marine deposits, is called Mississippian in North America, Dinantian in Europe, and Fengningian in China, respectively. The younger deposits are characterized by coal-rich, mixed marine and continental deposits in North America and Europe, and called Pennsylvanian and Silesian, respectively. The younger deposits in China, the Hutianian, are dominated by marine facies. According to the clear two-unit characteristics of the Carboniferous, the Subcommittee on Carboniferous Stratigraphy of the International Commission on Stratigraphy voted for two subsystems for the Carboniferous in 1998 and 2000, i.e., the Mississippian and the Pennsylvanian. This is the only period that contains sub-periods in the International Chronostrati-

graphic Chart. Although the Carboniferous has long been well studied in Western Europe and North America, the two regions lack continuously deposited marine successions, which hinders the establishment of Global Stratotype Sections and Points (GSSPs) for a global chronostratigraphic framework. However, near-continuous, marine carbonate successions are developed in the Russian platform, South Urals, North Spain, and South China, which potentially provides ideal outcrops for establishing a global Carboniferous chronostratigraphy.

2. Brief history of Carboniferous chronostratigraphic studies

2.1 Establishment of international chronostratigraphic chart of the Carboniferous

The Carboniferous was named after coal-bearing strata in the North England by Conybeare R D and Phillips W in 1822 (see Ramsbottom, 1984). Afterwards, a number of stages were established prior to the beginning of the 20th century in west and east Europe, such as the Namurian in South Belgium, the Westphalian in West Germany, and the Stephanian in middle to southern France. These represent widely distributed coal-bearing paralic strata in West Europe. The Tournaisian and Visean strata in South Belgium, and the Serpukhovian, Moscovian, and Gzhelian strata in the Moscow Basin of Russia, represent marine carbonate strata.

Munier and Lapparent (1893) established a Carboniferous chronostratigraphic framework based on marine strata of East Europe, including (in order) the Dinantian, Moscovian, and Uralian stages, the latter two of which correlate to the Westphalian and Stephanian of West Europe, respectively. This chronostratigraphic scheme was, however, not commonly used, and the Moscovian and Uralian are now used for totally different strata. Instead, a Carboniferous chronostratigraphy representative of West Europe was adopted in the first Carboniferous Congress held in 1927, which includes the lower Carboniferous Dinantian and the upper Carboniferous Namurian, Westphalian, and Stephanian stages (see Wagner and Winkler Prins, 2016).

In the 7th Carboniferous Congress held in Krefeld of Germany, 1971, the Carboniferous was subdivided into the Dinantian and Silesian subsystems, representing the previous Lower and Upper series, respectively. The Dinantian includes the Tournaisian and Visean stages, and the Silesian contains the Namurian, Westphalian, and Stephanian stages. With the increasing demand for global correlation, studies of the Carboniferous marine successions of East Europe and North America have been better recognized worldwide. By the 8th Carboniferous Congress, held in Moscow of Russia in 1975, the chairman of the congress, Bouroz A first proposed the currently widely accepted stratigraphic scheme,

which includes the Mississippian and Pennsylvanian subsystems, the former containing the Tournaisian, Visean, and Serpukhovian stages in ascending order, and the latter comprising the Bashkirian, Moscovian, Kasimovian, and Gzhelian stages in ascending order. The scheme, based on marine successions from West Europe, Russia, and North America, had been widely recognized.

The Subcommittee on Carboniferous Stratigraphy of the International Commission on Stratigraphy voted for the Mississippian and Pennsylvanian subsystems for the Carboniferous in 1998. In the next year during the 14th Carboniferous Congress held in Calgary of Canada, chairman Heckel P proposed the use of the 1975 scheme as the international Carboniferous chronostratigraphy (Heckel, 2001), and this was later officially approved by the Subcommittee on Carboniferous Stratigraphy. Although the international Carboniferous chronostratigraphy was established, almost every country was still using their own regional chronostratigraphy. The stage-level chronostratigraphy of West Europe, Moscow Basin and Urals of Russia, and Mid-continent of U.S. has been studied in detail, but these frameworks are still difficult to use for global correlation.

In the established Carboniferous chronostratigraphic chart, the Tournaisian and Visean stages are both named after marine successions in Belgium (see Hance et al., 2006a, 2006b). The Serpukhovian, Moscovian, and Gzhelian stages were proposed based on strata from the southern part of the Moscow Basin by Nikitin (1890). The Bashkirian Stage was established by Semikhatova (1934) based on strata of the Bashkirian Mountains in the South Urals of Russia. The Kasimovian was originally included as a part of the Moscovian Stage by Nikitin (1890), and later renamed as Kasimovian Stage by Teodorovich (1949).

The GSSP of the base of Carboniferous and the Tournaisian was approved in the La Serre section of France early in 1990 by the International Union of Geological Sciences (IUGS). The Hasselbachtal section of Germany and the Nanbiancun section of China were selected as the auxiliary stratotypes. The Mississippian-Pennsylvanian boundary, i.e., the base of the Bashkirian, was approved by the IUGS in 1996, and the GSSP is located in the Arrow Canyon section of Nevada, US. The GSSP of the Visean approved in 2008 is located in the Pengchong section of the Liuzhou City, Guangxi, China (Devuyt et al., 2003; Hou et al., 2013). The remaining 4 stages, including Serpukhovian, Moscovian, Kasimovian, and Gzhelian, have no GSSPs so far.

2.2 History of Carboniferous chronostratigraphy of China

Establishment and application of the Chinese Carboniferous stratigraphic divisions were initiated by the first generation of Chinese geologists including Ting V K, Wong W H, Lee J

S, Chao Y T and others. Ting V K named the Carboniferous strata in East Yunnan and West Guizhou, South China as the Weining system in 1914. The result, however, was published 22 years later (Ting and Grabau, 1936). After investigations of the strata in South China by Ting V K and others, Wong W H, Lee J S, and Chao Y T established the Taiyuan and Penchi series, which were coeval to the Weining system, based on investigations on the coal-bearing strata in North and Northeast China in 1925 and 1926. They subdivided the late Carboniferous strata into, in ascending order, the Penchi, Taiyuan, and Shansi series. Later in 1931, based on investigations on the Carboniferous in North Guangxi and South Guizhou regions, Ting established the Fengningian system, including Aikuan and Tang series, which are again subdivided into Gelaohu, Tangbagou, Jiushi, and Shangsi stages, in ascending order. Together with these geological studies, paleontological studies also made significant progress. Many paleontologists including Lee (1927), Chen (1934a, 1934b), Chao (1927, 1928, 1929), Grabau (1936), and Yin (1932, 1933) published papers on Carboniferous fossils such as fusulinids, brachiopods, and mollusks. These works provided substantial paleontological data for Ting V K and Grabau to propose the Carboniferous subdivision scheme of China during the 16th International Geological Congress in 1933 (Ting and Grabau, 1936). They divided the Carboniferous into two subsystems, using the American Mississippian and Pennsylvanian nomenclature, which contain lower, middle, and upper parts. The Aikuan and Tang series were correlated with the European Tournaisian and Visean, respectively. This subdivision scheme provided a basis for later studies on the Carboniferous of China, especially for the establishment of series- and stage-level chronostratigraphy.

During the 1950s to 1970s, the Carboniferous subdivision of Chinese stratigraphy was adopted similar to the three-part scheme of the former Soviet Union; the previous Upper Carboniferous was subdivided into two series, namely middle and upper Carboniferous Series. The Lower Carboniferous series and stages were retained the same. Yang et al. (1962) summarized the Carboniferous litho-, bio-, and chronostratigraphy of China, proposing three series; the Lower Carboniferous series was again subdivided into Aikuan and Tang stages, whereas the middle and upper Series were not further subdivided. Since the 1980s, the main progresses on the Carboniferous subdivision of China lies mainly on the following events. First, the Carboniferous was re-subdivided into two series, without opposed opinion (Yang et al., 1979; Hou et al., 1982), which is consistent with the Carboniferous depositional sequences and biotic evolution. Second, Chinese researchers were actively competing for the GSSPs of the Carboniferous stages. The auxiliary stratotype of the base of the Carboniferous is located in the Nanbiancun section of the Guilin City, Guangxi (Yu, 1988).

With collaboration with foreign researchers, the GSSP of the Viséan was ratified in Guangxi in 2008. Third, the 11th and 16th International Carboniferous (and Permian) Congress were held in Beijing, 1987 and Nanjing, 2007, respectively.

The regional Carboniferous chronostratigraphy of China was gradually established during the 1980s to 1990s, based mainly on the strata in Guizhou, Guangxi, Yunnan and Hunan; most of the Chinese stages were named after lithostratigraphic units (Rui et al., 1987; Zhang, 1987, 1988; Zhang et al., 1988). Among these stages, the Luosuan Stage was established based on a conodont-rich carbonate slope succession (Rui et al., 1987); the rest of the regional stages were all based on shallow-water successions (Wang and Jin, 2000). Since the beginning of this century, no new stage names have been proposed. Instead, Chinese researchers focused mainly on the biostratigraphy of deep-water successions, high-resolution correlation with other regions globally, and the search and correlation of index fossils for the GSSPs of the four unrated stages.

The regional Carboniferous chronostratigraphy of China includes two subsystems, i.e., the lower Fengningian Subsystem and the upper Hutianian Subsystem, which are correlative to the Mississippian and Pennsylvanian, respectively. The Fengningian Subsystem was subdivided into two series, i.e., Aikuanian and Tatangian series, and the Hutianian Subsystem into Weiningian and Mappingian series. The Carboniferous of China includes 8 stages, i.e., Tangbagouan, Jiusian, Shangshian, Dewuan, Luosuan, Huashibanian, Dalaun, and Xiaodushanian stages in ascending order (Figure 1; Jin et al., 2000; Wang and Jin, 2003, 2005).

3. Integrative Carboniferous stratigraphic time scale of China

Biostratigraphy is the basis for establishing Carboniferous chronostratigraphy, which is the requirement in the “International Stratigraphic Guide” published by the International Commission on Stratigraphy. The basic working unit (stage) of chronostratigraphy is defined by the First Appearance Datum (FAD) of descendant species of an evolutionary lineage. Recently, chemo-, magno-, and event-stratigraphy and radiogenic ages have been utilized to supplement global chronostratigraphic framework. Among the four stages without GSSPs, the base of the Gzhelian will be the FAD of the index fossil conodont *Idiognathodus simulator*. Index fossils for the other three stages (i.e., Serpukhovian, Moscovian, and Kasimovian) are still under discussion, but will most likely be based on conodonts (Richards, 2013). The nearly continuously deposited marine carbonate slope successions in South China, Russian Urals, and North Spain provide ideal sections to search for these GSSPs. The carbonate slope successions in South China formed at a rela-

tively rapid sedimentation rate, have continuous outcrops, and yield abundant conodonts with almost complete lineages.

3.1 Biostratigraphic framework

Conodonts are the primary fossil group for subdivision of Carboniferous chronostratigraphy. Foraminifera are secondary, and are regarded as the key bridge for correlation between carbonate slope and shallow-water platform successions. Ammonoids are another index fossils for carbonate slope successions and are regarded as the key fossil for the subdivision and correlation of the early Carboniferous. Brachiopods and rugose corals also play a role in subdivision and correlation of shallow-water platform successions.

3.1.1 Conodont biostratigraphy

The thick carbonate strata of the Naqing section in Guizhou, South China were rapidly deposited in a carbonate slope setting during the Carboniferous. A nearly complete Carboniferous conodont succession was recognized at this section. The Naqing section has been recently selected as the GSSP candidate for the four unrated Carboniferous stages. The conodont biozones established in the Naqing section have been applied as the standard Carboniferous conodont zonation of China, and is becoming more important globally. The conodont zones of China mostly followed those of the Russian Platform, Donets Basin, Urals, and North America, where Carboniferous conodonts have been studied and zoned for a long time. In recent decade, significant progress has been made on the conodont biostratigraphy of the Naqing section, which is noted internationally. Twenty-six conodont zones represented the most complete conodont succession in one single section, have been recognized in the Naqing section. Adding 11 conodont zones established from other sections in South China, 37 Carboniferous conodont zones have been established in China and can be correlated with other regions globally (Figure 2).

3.1.2 Foraminifera biostratigraphy

Non-fusulinid foraminifers are important fossils in Mississippian carbonate successions. The biostratigraphy and biozones established based on foraminifers are useful in regional and global correlations, given their rapid evolution. For example, the FAD of *Eoparastaffella simplex*, in the lineage of “*E. ovalis* group” to *E. simplex*, has been officially approved as the biostratigraphic criterion to define the base of the Viséan Stage (Devuyst et al., 2003). After decades of research on Chinese Mississippian foraminifera (Wang, 1983; Lin et al., 1990; Wu, 2008; Hance et al., 2011; Sheng, 2016; Sheng et al., 2018), there are 12 foraminiferal zones, three in the Tournaisian, five in the Viséan, and four in the Serpukhovian. However, compared with European zones

Age (Ma)	Standard chronostratigraphy				Russia				Western Europe		North America		China	
	System	Sub-system	Series	Stage	Moscow Basin		Urals		Stage	Substage	Stage	Formation	Sub-system	Series
					Stage	Substage	Substage	Substage						
295	Permian	Cis-Taiian	Upper	Asselian	Kholodnolozhskian	Shikhkhanian	Autunian	Kuzel	Wolfcampian	Permian	Wolfcamp	Fenglingian	Permian	Zisongian
300				Gzhelian	Melekhovian Noginskian Pavlovoposadskian Dobryatinskian	Nikolskian Martukian Azantashian	Stephanian	Stephanian C	Wabansee Shawnee Douglas	Xiaodushanian				
305	Pennsylvanian	Upper	Kasimovian	Dorogomilovian Khamovnikian Krevyakkian	Kerzhakovian Lomovskian	Stephanian B	Stephanian	Stephanian B	Missourian	Hurtianian	Lonsing Kansas City Pleasanton	Fenglingian	Hurtianian	
310			Moscovian	Myachkovian Podolskian Kashirian Verian	Tashlian Zilimian	Stephanian A	Stephanian A	Desmoinesian	Marmaton Cherokee		Dalaun			
315	Carboniferous	Middle	Lower	Bashkirian	Melekestian Chermshtankian Prikamian	Imenditashvian Soloncian Asataurian Tashastian	Westphalian	Bolsovian (C)	Atokan	Hurtianian	Atoka	Fenglingian	Hurtianian	
320						Severokelmenian Krasnopolyan Voznesenskian	Akavassian Kamennogor Bogdanovkian	Namurian	Duckmanian (B) Langsettian (A) Yeadonian Marsdenian Kinderscoutian Alportian Chokiarian		Morrowan			Winslow Bloyd Hale
325	Carboniferous	Upper	Lower	Serpukhovian	Zapalyubian	Chernyshevskian	Namurian	Arnsbergian	Grove Church Kinkaid	Fenglingian	Grove Church Kinkaid	Fenglingian	Hurtianian	
330						Protvian Steshevian Tarusian	Khudolazian Sunturian	Pendleian	Yeadonian Marsdenian Kinderscoutian Alportian Chokiarian		Morrowan			Winslow Bloyd Hale
335	Carboniferous	Middle	Lower	Visean	Venevian	Bogdanovichian	Visean	Asbian	Chesterian	Fenglingian	Grove Church Kinkaid Degonia to Palestine Menard	Fenglingian	Hurtianian	
340						Mikhailovian	Averinian	Brigantian	Yeadonian Marsdenian Kinderscoutian Alportian Chokiarian		Morrowan			Winslow Bloyd Hale
345	Carboniferous	Middle	Lower	Visean	Aleksinian	Kamenskouralskian	Visean	Holkerian	Meramecian	Fenglingian	St. Louis Salem	Fenglingian	Hurtianian	
350						Tulian	Zhukovian	Asbian	Yeadonian Marsdenian Kinderscoutian Alportian Chokiarian		Morrowan			Winslow Bloyd Hale
355	Carboniferous	Lower	Lower	Tournaisian	Bobrikian	Usigrekhovkian	Tournaisian	Arundian	Osagean	Fenglingian	Upper Warsaw Lower Warsaw Keokuk	Fenglingian	Hurtianian	
360						Radaevkian	Burlin Obruchevkian Kosvian	Chadian	Osagean		Upper Warsaw Lower Warsaw Keokuk			Meramecian
360	Devonian	U.	U.	Famennian	Tournaishian	Pershinian Rezhian upper lower	Tournaisian	Ivorian	Kinderhookian	Fenglingian	Burlington Fern-Glen Meppen	Fenglingian	Hurtianian	Tangbagouan
360						Gumerovian	Gumerovian	Famennian	Hastarian		Chataquan			Louisiana

Figure 1 International Carboniferous chronostratigraphic subdivision and correlation. Data based on Wagner and Winkler Prins (1991, 2016); Alekseev et al. (1996, 2004), Wang and Jin (2003) and Richards (2013).

(Figure 3), Chinese foraminiferal zones from the Tournaisian and Viséan stages need further work.

Fusulinids are the dominant marine fossil of shallow-water platform strata around the world. Due both to global tectonics that caused closing of the equatorial seaway, and to frequent changes in global sea level during this time, provincialism of benthic fusulinids became pronounced, which makes it difficult for correlation between Eurasian fusulinid biozones and those from North American. However, correlation of fusulinid biostratigraphy within Eurasia is certainly possible. There is a long history of research on Chinese Carboniferous fusulinid biostratigraphy (see Wang and Jin, 2003), and integrative works in recent years include Zhang et al. (2010) and Shi et al. (2012). Around the world, studies of fusulinids from the Donets Basin and Russian Platform are the most detailed, and the associated zones are generally divided by the evolution of species, although in the past, Chinese fusulinid zones were partly named for genera (e.g., Jin et al., 2000). This paper follows the 12 Pennsylvanian fusulinid zones proposed in Zhang et al. (2010) (Figure 4).

3.1.3 *Ammonoid biostratigraphy*

The macrofossil ammonoids can easily be recognized in the field, and they record relatively distinct evolutionary stages that allow for low-resolution chronological designation. For this reason, in the early research of Carboniferous biostratigraphy, ammonoids served as a very important tool in subdivision and correlation of strata, especially in Western Europe (Schmidt, 1925; Korn and Klug, 2015). The restricted distributions of many ammonoid species have been recognized by further research and it turns out that the correlation between two regions/continents far away from each other can only be roughly done at genus level. In addition, the distribution of ammonoids is also controlled by sedimentary facies, e.g., rarely found in shallow water facies. The localities for Carboniferous ammonoids in China are mainly in Xinjiang, Gansu, Ningxia, Tibet (Xizang), Guizhou, and Guangxi (Yang, 1978; Ruan, 1981a, 1981b; Sheng, 1983; Ruan and Zhou, 1987; Liang and Wang, 1991). They are most productive within limestone, calcareous sandstone or marl, as well as the calcareous concretions or lens, which are usually not fit for continuous sampling. Since many species of ammonoids co-occurring, the ammonoid zonation in China is much rougher than those based on the single section or better lithological correlations in Western and Central Europe. Except for the study of the Tournaisian ammonoids in Xinjiang (Zong et al., 2015), no other significant progress has been made for nearly two decades. Therefore, in this paper, we still follow the composite zonations, summarized by Wang and Jin (2003), with minor revisions of the indexes and their ranges. Thirteen Carboniferous ammonoid zones are recognized in China (Figure 4).

3.1.4 *Brachiopod biostratigraphy*

Brachiopods are an important marine fossil group in Carboniferous strata. They are widely distributed in many types of ecological environments and sedimentary facies. They are most commonly found in shallow water carbonate facies, as well as in turbidites or slumps in shelf facies. Mississippian brachiopods record high rates of evolution and diversification, resulting in distinct palaeobiogeographic provinces. Thus, the brachiopod zonation has relatively high resolution and is useful in stratigraphic subdivision and intra-provincial correlation. In the Pennsylvanian, however, their diversity decreased and the rate of evolution slowed, which resulted in reduced biostratigraphic resolution. A succession of 10 brachiopod assemblage zones was recognized in the Carboniferous in South China (Figure 4).

3.1.5 *Rugose corals*

Rugose corals are one of the dominant fossil groups commonly found in shallow marine carbonate facies in the Carboniferous. Similar to the brachiopods, they also demonstrate high rate of diversification and evolution in the Mississippian. Yu (1931, 1933) established a biostratigraphic succession of four rugose coral zones for the Mississippian of southern Guizhou, in ascending order, the *Cystophrentis*, *Pseudouralinia*, *Thysanophyllum*, and *Yuanophyllum* zones. This coral zonation scheme has been widely used afterward in stratigraphic subdivision and correlation of shallow-water facies. In the late 20th century, rugose coral biostratigraphic studies were carried out extensively in South China and related areas (see Wang and Jin, 2003). As a result, some areas, such as western Guizhou and eastern Yunnan (Wu and Zhao, 1989), received much attention and provided abundant data for research subject. Based on the accumulated data of several decades, we propose a rugose coral succession of 10 zones (Figure 4).

3.1.6 *Biostratigraphic framework for regional chronostratigraphy in China*

Given the variable sedimentary facies in different regions of China, it is practical to retain Chinese stages for the time being, although it is necessary to use the global standard chronostratigraphy whenever possible. This study follows the subdivision of the Carboniferous proposed by Jin et al. (2000), which includes 2 subsystems, 4 series, and 8 stages (Figures 1, 4). The biostratigraphic scheme of those stages is briefly summarized as follow (Figure 4). The Tangbagouan Stage can be correlated to the Tournaisian. Biostratigraphy of shallow-water successions is represented by the Dushan area, and biostratigraphy of the deep-water successions by the Wangyou and Muhua formations in the Changshun region. The Jiusian Stage is correlative to the lower part of the Viséan, including two rugose coral zones, one brachiopod zone, and two conodont zones. The base of the Jiusian Stage is

Chrono-stratigraphy	Belgium and North France		South China		
	Foraminifera	Rugose coral	Foraminifera	Rugose coral	
Carboniferous	MFZ16 (<i>Tubispirodiscus leckwijcki</i>)	RC9	<i>Monotaxinoides transitorius</i>	<i>Aulina rotiformis</i>	
			<i>Bradyina cribrostomata</i>		
			<i>Eostaffellina paraprotvae</i>		
			<i>Janischewskina delicata</i> / <i>Plectomillerella tortula</i>		
	MFZ15(<i>Janischewskina typica</i>)	RC8(<i>Lonsdaleia</i>)	<i>Asteroarchaediscus baschkiricus</i>	<i>Yuanophyllum</i>	
	MFZ14(<i>Howchinia bradyana</i>)	RC7(<i>Dibunophyllum</i>)			
	MFZ13(<i>Neoarchaediscus</i>)		RC6(<i>Lithostrotion araneum</i>)		<i>Archaediscus krestovnikovi</i>
	MFZ12(<i>Pojarkovella nibelis</i>)	RC5(<i>Siphonodendron</i>)			
	MFZ11(<i>Uralodiscus rotundus</i>)				RC4 (<i>Sychnoelasma hawbankense</i>)
	MFZ10(<i>Planoarchaediscus</i> / <i>Ammarchaediscus</i>)	<i>Viseidiscus monstratus</i>	<i>Parazaphriphyllum</i>		
	MFZ9(<i>Eoparastaffella simplex</i>)	<i>Eoparastaffella ex gr. ovalis</i>		K.-P. interval	
	MFZ8(<i>Eoparastaffella M1</i>)		<i>Dainella gumbeica</i>		
	MFZ7(<i>Darjella monilis</i>)	RC3(<i>Caninophyllum patulum</i>)		<i>Plectogyra komi-Granuliferella complanata</i>	<i>Keyserlingophyllum</i>
	MFZ6(<i>Tetrataxis</i>)		RC2(<i>Siphonophyllia rivagensis</i>)		<i>Uralinia tangpakouensis</i>
	MFZ5(<i>Paraendothyra nalivkini</i>)	RC1(<i>Coniophyllum</i>)			C.-U. t. interval
	MFZ4(<i>Spinochernella brencklei</i>)		DFZ8	RC0	<i>Quasiendothyra konensis dentata</i>
	MFZ3(<i>Pal. tchernyshinensis</i>)				
MFZ2(<i>Septabrunkiina minuta</i>)					
MFZ1(<i>Unilocular</i>)					
Devonian					

Figure 3 Mississippian foraminiferal and rugose coral zonations of China and their correlation with western Europe (Belgium and North France). Data of western Europe are from Poty et al. (2006). Pal.=Palaeospiroplectamina; K.-P. interval = Keyserlingophyllum-Parazaphriphyllum interval; C.-U. t. interval=Cystophrentis-Uralinia tangpakouensis interval.

defined by the FAD of *Eoparastaffella simplex*. The Shangsian Stage is correlative to the upper part of the Viséan. The base of the Shangsian Stage is defined by the FAD of either the rugose coral *Yuanophyllum* or brachiopod *Vitilproductus groberi-Pugilis hunanensis* in shallow-water successions, and by the FAD of conodont *Gnathodus bilineatus bilineatus* in deep-water successions. The Dewuan Stage can be correlated to the international Serpukhovian, the base of which is roughly defined by FAD of rugose coral *Aulina rotiformis* or brachiopod *Gigantoproductus edelburgensis* in shallow-water facies, and by the FAD of conodont *Lochriea zieglerei* in deep-water facies. The base of the Luosuan Stage is the same as that of the Bashkirian, and is defined by the FAD of conodont *Declinognathodus noduliferus* s.l. and the fusulinid *Millerella marblensis*. The Hua-shibanian Stage is generally correlated to the fusulinid *Pseudostaffella* zone, including one brachiopod zone and three conodont zones. The Dalaun Stage is correlative to the previous fusulinid *Profusulinella* zone and *Fusulina-Fusulinella* zone (Jin et al., 2000), which is now subdivided into 6 fusulinid zones (Zhang et al., 2010). The Xiaodushanian Stage, the base of which is correlative to that of the international stage Kasimovian, is defined by the FAD of fusulinid *Montiparus* or *Protriticites*, and by the disappearance of

Fusulina and *Fusulinella*. The upper boundary is defined by the FAD of *Pseudoschwagerininae*. The Xiaodushanian Stage includes 10 conodont zones.

3.2 Sequence and cyclo-stratigraphy

Development of depositional sequences and high-frequency cycles during the Carboniferous was closely related to the waxing and waning of Gondwanan glaciation (Ross and Ross, 1988; Li et al., 1997; Rygel et al., 2008; Ueno et al., 2013). The alternating occurrences of glacial-interglacial periods resulted in frequent and episodic eustatic changes, which led to development of cyclothem in low-latitude regions, including South China. During glacial periods, dramatic eustatic fall led to subaerial exposure, deposition of siliciclastic and dolostone units, carbonate carbon ($\delta^{13}\text{C}_{\text{carb}}$) and oxygen ($\delta^{18}\text{O}$) isotope anomalies, biotic extinction and turnover events, as well as disappearance of reefs (Wang et al., 2013).

Li et al. (1997) summarized the Carboniferous Depositional sequences (DS) of South and North China. Two third-order sequences were identified in the Tournaisian and Viséan in South China. Each of the Serpukhovian, Bashkirian, and Moscovian to Lower Kasimovian contains one third-

System		Chronostratigraphy			Conodont	Foraminifera	Ammonoid	Brachiopod	Rugose coral		
		Standard	China								
Sub-system	Stage	Sub-system	Series	Stage							
Carboniferous	Permian	Asselian 298.9 Ma	Chuan-shanian	Zisongian	Streptognathodus isolatus	Sphaeroschwagerina spaerica -Pseudoschwagerina uddeni	Properirites plummeri	Choristites jigulensis- Protanidanthus	Kepingophyllum		
			Mapin	Xiaodus-shanian	S. wabaunensis S. tenuialveus S. virgillus I. simulator I. nashuensis S. zethus I. eudoraensis I. turbatul I. magnificus	Triticites subcrassulus- T. noinskyi plicatus T. parvulus-T. umbonoplicatus Montiparus weiningica- M. longissima	Proudtenites				
	Pennsylvanian	Moscovian	Hulianian	Weiningian	Dalaun	Swadelina makhlinae Sw. subexceisa I. podolskensis Mesogondolella clarki- Mesogondolella donbassica Diplognathodus eile smerenis	Fu. cylindrica-Fu. quasifusulinoides Fusulina pakhrensis- Pseudostaffella paradoxa Fusulina lanceolata- F. vozhaensis Fusulinella obasa-F. apulchra Profusulinella aijutovica- Ta. latzenhoensis extensa Pr. priscoidea-Pr. parva Ps. composite-Ps. paraconpressa Pseudostaffella antiqua- Ps. antiqua posterior	Owenoceras Winslowoceras Branneroceras- Gastrioceras Bilinguites- Cancelloceras Reticuloceras Homoceras	Buxtonia grandis Alexania gratiodentalis- Nantanea mapingensis- Choristites latum	Nephelophyllum- Pseudotimania	
						Bashk-irlian	Huashi-banian	"S." expansus M2 "S." expansus M1 I. primulus Neognathodus symmetricus Idiogonathodus sinuatus Declinognathodus noduliferus s.l.	Millerella marbiensis Monotaxinoides transitorius Bradyina cribrostomata Eostaffella paraprotvae Janishevskina delicata /Plectomillerella tortula		Choristites mansuyi -Semicoistella panxianensis
		Vissean	Fengningian	Tatangian	Shanghsian	Jiusian	Lochriaea nodosa	Asteroarchaediscus baschkiricus Archaeodiscus krestovnikovi Paraarchaediscus koktjubensis Viseidiscus monstratus Eoparasstaffella simplex	Goniatites	Gigantoproductus moderatus Vittilproductus groberi Pugilis humanensis Delepinea subcarinata- Megachonetes zimmermanni	Yuanophyllum Kueichouphyllum sinense-Dorlodotia Parazaphriphyllum
							Luosuan	Dewuan	G. postbilineatus G. boilandensis Lochriaea ziegleri	Ammonellipsites Pericyclus Gattendorfia Wocklumeria	Gigantoproductus edelburgensis- Gondolina-Striatifera Marginifera tenuistriata- Goniophoria carinata
	Devonian	Famennian	Tournaisian	Alkuanian	Tangba-gouan	Lochriaea bilineatus Lochriaea commutata Pseudognathodus homopunctatus	Eoparasstaffella ex gr. ovalis Dainella gumberica Plectogyra komi- Granuliferella compianata Quasiendothyra konensis dentata	Ammonellipsites Pericyclus Gattendorfia Wocklumeria	Finospirifer shaoyangensis Eochoristites- Martiniella Unispirifer- Yanguania Schuchertella gelaensis	K.-P. interval Keyserlingophyllum U. tangpakouensis C.-U. t. interval Cystophrentis	
						346.7 Ma	Upper	Shaodongian	Siphonodella praesulcata		
		Mississippian	Shanghsian	Fengningian	Tatangian	Jiusian	Scalognathodus anchoralis -G. pseudosemiglaber G. typicus- Protognathodus cordiformis G. typicus-G. cuneiformis Si. isosticha-U Si. crenulata Lower Si. crenulata Si. sandbergi Si. sulcata Si. duplicata U				
							323.2 Ma	Dewuan			

Figure 4 Carboniferous biostratigraphic scheme of China. See Figure 2 and Figure 3 for conodont and rugose corals abbreviations, respectively. T. = Triticites, M. = Montiparus, Fu. = Fusulina, F. = Fusulinella, Pr. = Profusulinella, Ps. = Pseudostaffella.

order sequence. The upper Kasimovian to Gzhelian has two third-order sequences. In North China, the Mississippian is missing, and the Pennsylvanian is characterized by alternating shallow-marine and continental deposits. The third-order sequences can be correlated to those of South China (Li et al., 1997). The second- and third-order sequences of the Carboniferous can be correlated between South China, Europe, and North America. High-frequency sequences are well developed in the Moscovian to Gzhelian worldwide in low-latitude regions (Ross and Ross, 1987; Li et al., 1997). Recently, Ueno et al. (2013) studied high-resolution Pennsylvanian cyclothems in the Zongdi section, Ziyun, Guizhou, South China, using fusulinid biostratigraphy. A total of 21 depositional sequences (DS), separated by subaerial exposure surfaces, were recognized in Moscovian (8 DS), Kasimovian (5 DS), and Gzhelian (8 DS) strata. The duration of each sequence is about 400–450 ka, consistent with an eccentricity driver (Ueno et al., 2013). These cyclothems can be well correlated to those developed coevally in the Mid-continent of the U.S. (Heckel, 2008).

3.3 Event stratigraphy and reef evolution

Multiple global regression events, $\delta^{13}\text{C}_{\text{carb}}$ anomalies, biotic extinction, and turnover events occurred during the end-Devonian to mid-Carboniferous interval (Caplan and Bustin, 1999; Wang et al., 2013). The extensive development of Hangenberg sandstone units and occurrence of the Hangenberg extinction event were triggered by global significant regression event at the end of the Devonian, resulting in the dramatic decline and/or elimination of stromatoporoids, rugose corals, ammonoids, conodonts, and trilobites (Caplan and Bustin, 1999; Kaiser et al., 2016). Microbial mats in carbonate platform globally proliferated in the earliest Carboniferous (early Tournaisian), and can be traced across southern and northwestern China (Hou et al., 2011; Yao et al., 2016). During the middle Tournaisian, a distinct regression event occurred, characterized by deposition of siliciclastic and dolostone strata. This event is likely the sea-level fall at the Kinderhookian-Osagean transition in North America, which is accompanied by a positive shift in $\delta^{13}\text{C}_{\text{carb}}$ (Wang et al., 2013; Yao et al., 2015). Then, under the sea-level rise in the late Tournaisian, Waulsortian-like carbonate mud mounds developed at the Longdianshan area in Liuzhou City, Guangxi, South China, corresponding to the coeval Waulsortian mud mounds widely distributed in Europe and North America (Lees and Miller, 1985; Aretz et al., 2012). During the latest Tournaisian, a distinct sea-level fall occurred in South China, which resulted in exposed surfaces and siliciclastic deposition. This was the same regression event recorded in western Europe that is coincident with the disappearance of the late Tournaisian Waulsortian mud mounds, intensified meteoric diagenesis in shallow carbo-

nate facies, and the prominent negative excursion in $\delta^{13}\text{C}_{\text{carb}}$ (Aretz and Chevalier, 2007; Qie et al., 2011; Wang et al., 2013). In the latest Visean, another distinct regression event took place in South China, coinciding with that in Europe and North America, and it represents the initial glacial development on Gondwana continent during this time; it also resulted in a global positive shift in $\delta^{13}\text{C}_{\text{carb}}$ (Fielding et al., 2008; Grossman et al., 2008; Chen J T et al., 2016).

The reef evolutionary pattern is almost consistent between South China and other regions. The latest Visean regression event caused the disappearance of coral reefs, coral biostromes, and coral-microbial-bryozoan reefs in South China (Aretz and Webb, 2007; Yao and Wang, 2016). In the Serpukhovian, reefs greatly declined, and few coral, chaetetid biostromes, and microbial reefs are present in the Lianyuan and Lengshuijiang, Hunan Province (Liu, 2002; Gong et al., 2012). During the mid-Carboniferous boundary interval there was a distinct sea-level fall, development of exposure surfaces, and deposition of dolostones extensively across South China, in correspondence with both the wide development of glacial deposits on the Gondwana continent and a global positive shift in $\delta^{13}\text{C}_{\text{carb}}$ and $\delta^{18}\text{O}$ isotopes (Chen B et al., 2016). An important turnover event occurred in marine faunas and reef ecosystem during this transition from the Mississippian to the Pennsylvanian, characterized by the replacement of large dissepimented solitary corals by compound corals, and the evolution of small sized brachiopods (e.g., *Choristites*) replacing large-sized brachiopods (e.g., *Gigantoproductus*), the diversification in fusulinids into important index fossil in shallow-water facies, and the changes from metazoan reefs into algal reefs (Fan and Rigby, 1994; Gong et al., 2007; Wang et al., 2013; Yao and Wang, 2016).

3.4 Carbon isotope stratigraphy

Global carbon cycle perturbations in geological history are recorded by carbon isotopic compositions ($\delta^{13}\text{C}_{\text{carb}}$) of the whole rock or fossil calcite. Resulting isotopic chemistratigraphic curves are used as an important tool for stratigraphic division and correlation. Carbon isotope studies carried out in Europe and the United States sections revealed three major shifts in $\delta^{13}\text{C}_{\text{carb}}$ value for the Carboniferous: (1) a significant positive shift in the Tournaisian, with magnitude up to 5–7‰ (V-PDB), representing one of the largest $\delta^{13}\text{C}_{\text{carb}}$ excursions in the Phanerozoic (Mii et al., 1999; Saltzman, 2002; Saltzman et al., 2004); (2) a Serpukhovian decline (Saltzman, 2003; Batt et al., 2007); and (3) a positive $\delta^{13}\text{C}_{\text{carb}}$ shift again starting at the lowermost Pennsylvanian. The magnitude of the latter is different between Western Europe and United States records, with an increase in $\delta^{13}\text{C}_{\text{carb}}$ of ~1.5‰ in North America, but 3.0‰ in Europe (Mii et al., 1999; Bruckschen et al., 1999; Veizer et al., 1999; Saltzman, 2003).

The Tournaisian and Viséan carbon isotope records for South China are mainly based on the data from carbonate platform sections, which may be influenced by meteoric diagenetic alteration. The middle Tournaisian positive $\delta^{13}\text{C}_{\text{carb}}$ shift was well identified in the Longan section, an isolated carbonate platform succession in Guangxi (Qie et al., 2011), and the Malanbian section situated at the near-shore shallow-water setting in Hunan (Yao et al., 2015). The $\delta^{13}\text{C}_{\text{carb}}$ values increase from 0 to 6‰ in the Malanbian section, but only increase from 0 to 3‰ in the Longan section. Local environmental or hydrogeographic differences may explain this variable magnitude (Yao et al., 2015). The Viséan to Serpukhovian carbon isotope record from the Longan section shows similar trends to that of the Naqing section (Figure 5). However, distinct differences in $\delta^{13}\text{C}_{\text{carb}}$ values exist in the two sections, which might have resulted from chemical differences in water mass associated with ocean circulations or water depths between the two sections.

The Naqing Section is located in the southwest part of Luodian County in southern Guizhou, where a continuous Carboniferous to Permian carbonate succession with abundant conodont elements crops out. The section is thought to have been deposited in a carbonate slope setting of the Luodian basin in the Dian-Qian-Gui Sea. The carbon isotope record from the Naqing section shows slight variation in $\delta^{13}\text{C}_{\text{carb}}$ values (~3‰) from the Viséan to Serpukhovian, a gradual increase from the earliest Bashkirian to latest Moscovian (~4‰), a short-lived period of lower values (~2‰) near the Kasimovian-Gzhelian boundary interval, and a rapid rise to 5.5‰ in the Gzhelian (Figure 5; Buggisch et al., 2011; Chen et al., 2018). Although the direct link between $\delta^{13}\text{C}_{\text{carb}}$ changes and ice volumes is not straightforward, the high $\delta^{13}\text{C}_{\text{carb}}$ values in the Gzhelian is interpreted to reflect extensive ice sheets expansion for the late Paleozoic ice age (Buggisch et al., 2011). The increase in $\delta^{13}\text{C}_{\text{carb}}$ values is generally regarded as an indicator of increasing organic carbon burial, which would result in lowering of atmospheric CO_2 concentrations and climatic cooling (Mii et al., 1999; Saltzman, 2002, 2003; Saltzman et al., 2004; Buggisch et al., 2008; Chen et al., 2018). It is worth noting that $\delta^{13}\text{C}_{\text{carb}}$ profiles of many platform successions show low values from Gzhelian to lowermost Permian (Buggisch et al., 2011), which are attributed to diagenetic alteration due to platform exposure to meteoric water during sea-level fall as a consequence of increased glaciation (Buggisch et al., 2011).

3.5 Oxygen isotope stratigraphy

The oxygen isotope ratios preserved in fossil skeletons (calcite or phosphate) are dependent on the oxygen isotopic composition and temperature of seawater in which organ-

isms lived. Thus, ancient seawater temperature can be inferred by measuring $\delta^{18}\text{O}$ values in fossil skeletons if their primary oxygen isotopes signal is preserved and the ancient seawater $\delta^{18}\text{O}$ value is known or can be reasonably assumed. The Carboniferous–Permian is one of the most notable “icehouse” periods in the Earth history. Reconstructing fossil $\delta^{18}\text{O}$ records for this critical time can provide information about changes in ice volume and seawater temperature, both of which are key parameters to define a glaciation magnitude.

Grossman et al. (2008) compiled Carboniferous $\delta^{18}\text{O}$ data of brachiopod shells from North America and the Russia platform. In the North American record, they found a ~3‰ (V-PDB) increase in Tournaisian to middle Viséan strata, followed a further ~1‰ rise at the Serpukhovian to Bashkirian transition. $\delta^{18}\text{O}$ values remain relatively stable with values from -3‰ to -1‰ throughout the entire Pennsylvanian. Oxygen isotope record from the Russian platform shows a 3‰ increase at the Serpukhovian–Bashkirian transition. Buggisch et al. (2008) identified two major $\delta^{18}\text{O}$ positive shifts in the Mississippian of Europe and North America, as recorded by conodont apatite and brachiopod calcite one in the Tournaisian with magnitude of ~1.5‰ (V-SMOW) and the other in the Serpukhovian to Bashkirian transition with a magnitude of ~1‰ (V-SMOW). These increases in $\delta^{18}\text{O}$ values are interpreted as a record of continental ice sheet buildup and/or climatic cooling. Since ice preferentially absorb ^{16}O , lower temperatures and the buildup of ice sheets result in ^{18}O enrichment in seawater.

Recently, Chen B et al. (2016) reported a continuous $\delta^{18}\text{O}_{\text{apatite}}$ record spanning the late Viséan to Middle Permian from South China (Figure 5). They found the average $\delta^{18}\text{O}$ values slightly above 22.0‰ for the late Viséan, and a minor decrease to around 21.2‰ in the early Serpukhovian. These were followed by a prominent positive shift from 21.2‰ (early Serpukhovian) to the maximum value of 23.3‰ in the middle Bashkirian. The $\delta^{18}\text{O}$ values decrease to 22.0‰ at the Bashkirian–Moscovian boundary, and further decrease to 21.5‰ in the Gzhelian.

Overall, the Tournaisian and Serpukhovian–Bashkirian increases are two major oxygen isotope changes that can be identified in the Carboniferous $\delta^{18}\text{O}$ record. $\delta^{18}\text{O}$ values rise in the Tournaisian. High values in the Viséan are thought to maybe related to local aridification in North America (Grossman et al., 2008), but currently no coeval data is reported from the Russian platform and South China, and therefore whether this increase is of global significance or just a reflection of regional aridification still requires further data to confirm. The significant $\delta^{18}\text{O}$ increase in the Serpukhovian–Bashkirian boundary interval is demonstrated to have occurred widely and is interpreted as indicating the ice volume maximum for the late Paleozoic ice age (Chen B et al., 2016). Rising carbon and strontium isotopes ratios pre-

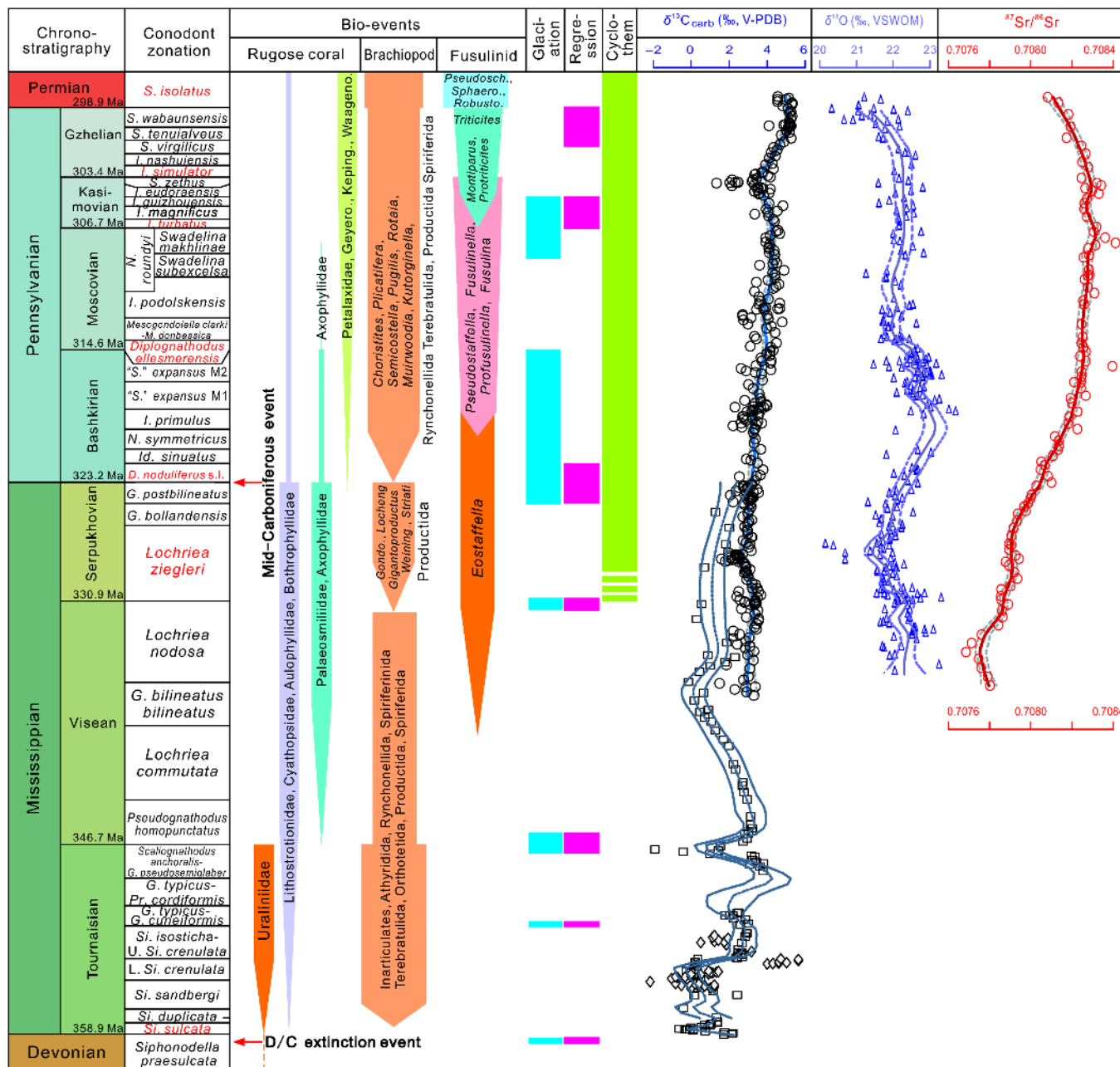


Figure 5 Carboniferous bio- and geo-events and chemostratigraphy of China. Bio-events, regression and cyclothem based on Wang et al. (2013); carbon isotope data from Qie et al. (2011) and Buggisch et al. (2011); oxygen isotope (conodonts) data from Chen B et al. (2016); strontium isotope (conodonts) data from Chen et al. (2018). See Figure 2 for conodont abbreviations. *Geyero.* = *Geyerophyllidae*, *Keping.* = *Kepingophyllidae*, *Waageno* = *Waagenophyllinae*, *Pseudosch.* = *Pseudoschwagerina*, *Sphaero.* = *Sphaeroschwagerina*, *Robusto.* = *Robustoschwagerina*.

served in brachiopod fossil shell or carbonate is in agreement with this interpretation. The former reflects an increase in the burial of organic carbon, and the latter indicates an enhancing of continent weathering rates, and both have the potential to trigger climate cooling, culminating in large-scale ice sheets buildups (Bruckschen et al., 1999; Grossman et al., 2008). Significant sea-level decline and exposure surfaces (Ross and Ross, 1987; Alekseev et al., 1996; Eros et al., 2012; Wang et al., 2013) are assumed to have resulted from

ice sheet build-up in high latitudes, and are widely found in uppermost Mississippian to lower Pennsylvania strata in North America, Russia, South China, as well as other low-latitude regions, which further reinforce this interpretation.

3.6 Strontium isotope stratigraphy

Given the long residence time (1–3 Myr) of strontium in the ocean relative to the short ocean mixing time (~1.5 ka),

seawater strontium is regarded as homogeneous at any given time. Thereby, strontium isotopes ($^{87}\text{Sr}/^{86}\text{Sr}$) can be used for stratigraphic correlation and dating, especially for intervals with simply rising or declining trends in $^{87}\text{Sr}/^{86}\text{Sr}$ (McArthur et al., 2012). Seawater $^{87}\text{Sr}/^{86}\text{Sr}$ is controlled mainly by inputs of more radiogenic isotopes from continental weathering and less radiogenic isotopes from hydrothermal exchanges through mid-ocean ridges. Therefore, seawater $^{87}\text{Sr}/^{86}\text{Sr}$ can reflect continental weathering, global tectonics, and paleo-climate conditions (e.g., Kump and Arthur, 1997; Chen et al., 2018). The Carboniferous $^{87}\text{Sr}/^{86}\text{Sr}$ curve was traditionally constructed using calcitic brachiopods from North America and East Europe (Bruckschen et al., 1995, 1999). However, due to the discontinuities and uncertainties in the Carboniferous of the two regions, and the possible diagenetic influence on brachiopod calcite, the existing $^{87}\text{Sr}/^{86}\text{Sr}$ values show great scatter.

Chen et al. (2018) analyzed $^{87}\text{Sr}/^{86}\text{Sr}$ of Carboniferous conodonts recovered from the Naqing section, Guizhou, South China. The conodont-based $^{87}\text{Sr}/^{86}\text{Sr}$ curve is largely consistent with previously published data, especially with those of brachiopods from the Panthalassic open-ocean setting (Brand et al., 2009) and of conodonts of the Russian Urals (Henderson et al., 2012). The Naqing section is a near-continuously deposited carbonate slope succession in the east Paleo-Tethys Ocean. This newly established $^{87}\text{Sr}/^{86}\text{Sr}$ curve based on conodonts is the most complete Carboniferous curve to date, which, when integrated with high-resolution conodont biostratigraphy, provides a reliable tool for global stratigraphic correlation.

The Carboniferous $^{87}\text{Sr}/^{86}\text{Sr}$ curve shows four phases: (1) a rapid fall from high values (~ 0.7084) around the Devonian-Carboniferous boundary to the nadir (~ 0.7076) in the middle Viséan, (2) a long-term rise from the middle Viséan to the high values (0.7083) in the middle-late Bashkirian (~ 318 Ma), (3) a ~ 15 Myr plateau ($318\text{--}303$ Ma), and (4) a relatively rapid fall from the early Gzhelian (~ 303 Ma) throughout the Permian (Veizer et al., 1999; Chen et al., 2018). The long-term rise in $^{87}\text{Sr}/^{86}\text{Sr}$ from the middle Viséan to Bashkirian was a result of increased continental weathering triggered by the Hercynian orogeny, and also partly from flourishing rainforests (intensifying weathering) (Chen et al., 2018). The $^{87}\text{Sr}/^{86}\text{Sr}$ plateau from the Bashkirian to lower Gzhelian would have been caused by sustained high weathering rate during the western propagation of the Hercynian orogeny from Europe to North America. The onset of rapid decline in $^{87}\text{Sr}/^{86}\text{Sr}$ in the early Gzhelian is consistent with floral restructions and the onset of widespread pantropic aridification in the Euramerica, implying that it was caused by decreased continental weathering. The continued decline in $^{87}\text{Sr}/^{86}\text{Sr}$ during the Permian might also have been related to basaltic eruption and opening of the Neo-Tethys.

4. Carboniferous lithostratigraphic provinces of China

The Carboniferous deposits of China are recognized in four provinces that have total 11 subprovinces (Jin et al., 2000; Wang and Jin, 2003). They are briefly described from north to south (Figure 6).

(1) The Junggar-Hinggan Province is subdivided, from west to east, into the Junggar, Inner Mongolia-Jilin and Hinggan subprovinces. In the Junggar subprovince, the Carboniferous consists mainly of siliciclastic, carbonate, and volcanic rocks, and the Inner Mongolia-Jilin subprovince contains thick siliciclastic strata and carbonate debris flow deposits. The Carboniferous fauna generally belong to the Boreal Realm, whereas paleoflora are found in the Angaran region.

(2) The North China-Tarim Province can be subdivided into the Tarim, North China, and Qilian-Helan Mt. subprovinces. This province generally contains stable shallow shelf facies with the Tethyan fauna and flora varying from Euramerican to Cathaysian affinities. Deep-water deposits occur in northern margin of the Tarim subprovince and southwestern margin of the North China subprovince.

(3) The Qiangtang-South China Province is subdivided into the Qiangtang-Hengduanshan subprovince and South China subprovince. This province contains a complete Carboniferous succession dominated by carbonate platform facies, with typical Tethyan fauna and floras varying from Euramerican to Cathaysian affinities.

(4) The Tibet-West Yunnan Province can be subdivided into the South Tibet, Gangdise, and West Yunnan subprovinces, which belonged to the northeastern margin of the Gondwana. The Mississippian is dominated by carbonate and siliciclastic shelf facies, whereas the Pennsylvanian is characterized by diamictite and volcanics, or missing along an unconformity. The fauna have Gondwanan affinities.

5. Index fossils and stratotypes of the unrati ed Carboniferous stages

Carboniferous stratotype research is hindered mainly by intense paleogeographic endemism, which was triggered by differential climates due to glacial-interglacial shifts and isolated geography due to global tectonics. Currently four stages have not yet been ratified for the GSSPs, including the Mississippian Serpukhovian and Pennsylvanian Moscovian, Kasimovian, and Gzhelian. Conodonts are the primary fossils for defining the stratotypes, with supplement of foraminifera (fusulinids) and ammonoids.

Although the index fossils for the base of the Serpukhovian has not been determined, the international working group for the Carboniferous focuses on the evolutionary

Chronostratigraphy		Junggar-Hinggan			Tarim-North China			Qiangtang-South China					Tibet-West Yunnan		
Standard	China	Balikun, Xinjiang	Central Jilin	Keping, Aheqi, Xinjiang	Jinyuan, Gansu	Taiyuan, Shanxi	Qamdo, Tibet	Dushan, Guizhou	Weining, Guizhou	Huanjiang, Guangxi	Shaodong, Hunan	Nanjing, Jiangsu	Gaize, Tibet	Shidian (Yudong), Yunnan	
P	Asselian	Zisongian												Dingjiazhai	
	298.9 Ma														
	Pennsylvanian	Gzhelian	Xiaodushanian												
		303.4 Ma													
		Kasimovian													
		306.7 Ma													
	Mississippian	Moscovian	Dalaun												
		314.6 Ma													
		Bashkirian		Luosuan											
		323.2 Ma													
Carboniferous	Serpukhovian	Dewuan													
	330.9 Ma														
	Visean	Shangsian													
			346.7 Ma												
		Tournaisian	Jiusian												
				358.9 Ma											
	D	Famennian	Shaodongian	Ke'ankuduk	Erdaogou (Silurian)	Kezirtag	Laojunshan	Fengfeng (Ordovician)	Wuqingna	Gelaohu	Rongxian	Menggongao	Wutong	Dazhaimen	

Figure 6 Subdivision and correlation of Carboniferous lithostratigraphic provinces in China

lineage of *Lochriea nodosa-L. zieglerei*, the FAD of the latter being regarded as the base of the Serpukhovian. There are currently two stratotype candidates. One is the Verkhnyaya Kardailovka section in the Russian Urals. Russian researchers reported the *Lochriea nodosa-L. zieglerei* lineage from this section. There is not many *L. zieglerei* specimens found to date, and few other typical Serpukhovian conodonts such as *L. senckenbergica* in the section. The typical Serpukhovian foraminifera *Asteroarchaediscus postrugosus* occurs about 7 m above the horizon that yields *L. zieglerei* in the section. The other candidate is the Naqing section, Guizhou Province, China, which consists of thin- to medium-bedded limestone. Almost each of the limestone bed contains abundant conodonts, about 100 conodont specimens on average in 1 kg limestone samples. The section yields the complete *Lochriea nodosa-L. zieglerei* lineage and abundant conodonts representative of the lower Serpukhovian, such as *L. cruciformis* and *L. senckenbergica*. The foraminifer that represents the base of the Serpukhovian, *Janischewskina delicata*, exists at 2.15 m above the FAD of *L. zieglerei*.

There is, unfortunately, no substantial research progress on the stratotype of the Moscovian. The Moscovian GSSP

working group has proposed four candidate concepts: (1) the FAD of the latter of the *Declinognathodus marginodosus-D. donetzianus* conodont lineage, (2) the FAD of the latter of the *Diplognathodus aff. orphanus-Di. ellesmerensis* conodont lineage, (3) the FAD of certain species of *Profusulinella*, and (4) the FAD of the latter of the *Verella-Eofusulina* lineage. The FAD of *D. donetzianus* is the closest level to the base of the traditional Moscovian Stage, but it is not present over wide areas and has not been found in China so far. The FAD of *Diplognathodus ellesmerensis* is also close to the base of the traditional Moscovian Stage and has a wide distribution. It has distinct, easily identified characteristics, and therefore holds more potential for global correlation (Qi et al., 2016). Because of distinct endemism, it would be difficult to search for a fusulinid species with worldwide distribution. Two stratotype candidates for the Moscovian Stage include (1) the Basu section in the South Urals, Russia that yields the conodont *Declinognathodus marginodosus-D. donetzianus* lineage as well as the fusulinid *Depratina prisca*, and (2) the Naqing section that yields abundant *Diplognathodus ellesmerensis* conodonts, as well as the fusulinid *Profusulinella* (Wang et al., 2011) but no specimens of the conodont *D.*

donetzianus.

The base of the Kasimovian may also be defined by conodonts, most likely either *Idiognathodus turbatus* or *I. sagittalis*. The FAD of the two is close, both about one substage higher than the traditional Kasimovian (Villa and Task Group, 2008). Recently, Rosscoe and Barrick (2013) defined a new species, *I. heckeli*, which is the direct ancestor of *I. turbatus*. The FAD of *I. heckeli* is closer to the base of the traditional Kasimovian (Ueno and Task Group, 2014). The FAD of *Swadelina subexcelsa* was recently proposed by Russian researcher as the boundary marker, which would mean reversion to the original definition of the Kasimovian Stage (Ueno et al., 2017). The FAD of fusulinids *Protriticites* and *Montiparus* can be used as an auxiliary fossil in shallow-water facies. There are currently three stratotype candidates: (1) the Usolka section in the Russian Urals yields *I. sagittalis* and fusulinids, but the section consists of alternative mudstone and limestone; (2) the Afanasievo section in the Russian Moscow Basin contains abundant fusulinid fossils including *Montiparus* and conodonts *I. sagittalis* and *Sw. subexcelsa*, in typical shallow-water facies containing several horizons of paleosols and hiatus (Goreva et al., 2009); and (3) the Naqing section in South China yields *I. swadei-I. heckeli-I. turbatus* lineage and conodont *Sw. subexcelsa* (Qi et al., 2012; Hu and Qi, 2017), as well as some fusulinids.

The base of the Gzhelian Stage is defined by the FAD of the conodont *Idiognathodus simulator* (Heckel et al., 2008), but the direct ancestor has not been found yet. *Idiognathodus eudoraensis* is regarded as having affiliation with *I. simulator*. The reason why it is difficult to establish the complete lineage might be due to the global regression at this time interval. There are currently three stratotype candidates. (1) The Usolka section in Russian Urals, which yields *I. simulator* and abundant fusulinid *Rauserites*. The boundary interval, however, contains intercalations of mudstone and limestone, not single lithofacies. (2) The Gzhel section in the Russian Moscow Basin, the type Gzhelian section, contains *I. simulator* and fusulinid *Rauserites rossicus*, possibly as auxiliary fossils. The section, however, represents shallow-water facies and there is a significant hiatus less than one m below the FAD of *I. simulator*. (3) The Naqing section in South China yields *I. simulator* as well as other abundant transitional conodonts between *I. eudoraensis* and *I. simulator*, which has great potential to find the direct ancestor of the latter. The fusulinids are, however, not rich in this section.

6. Summary and discussion

A Chinese Carboniferous chronostratigraphic framework has been established on the basis of detailed biostratigraphy mainly from South China. The high-resolution biostrati-

graphy reveals 37 conodont zones, 24 foraminifera (fusulinid) zones, 13 ammonoid zones, 10 brachiopod zones, and 10 rugose coral zones. It is practical to retain the regional Carboniferous chronostratigraphy of China, which includes 2 subsystems, 4 series, and 8 stages, which can be correlated with other regional frameworks such as Russian Moscow Basin, Russian Urals, and Midcontinent of United States. The chemo-, sequence-, cyclo- and event-stratigraphic studies of Chinese Carboniferous have also been carried out and correlated with those of other regions of the world.

Radiogenic age dating of Carboniferous rocks in China has been hindered because *in situ* volcanic ash layers have not been found. Geochronologic dates of the Carboniferous based on the U-Pb ID-TIMS are mainly from the Devonian-Carboniferous boundary interval from the Rhein region of Germany and the Pennsylvanian succession from the Donets Basin of Ukraine and South Urals of Russia (Trapp et al., 2004; Davydov et al., 2010; More recent and most precise dates in Myrow et al., 2014).

The Carboniferous magnetostratigraphy in China has made no progress, due mainly to remagnetization of the Carboniferous successions by multiple tectonic and thermal events in South China. In fact, there is no significant progress in Carboniferous magnetostratigraphy globally, not only because of re-magnetization but also due to the fact that the Permian-Carboniferous Reverse Superchron (PCRS) occurred from Pennsylvanian to the Early Permian (Tarling, 1991). Regardless, several normal polarities were recognized in the PCRS, and as many as 16 normal polarity zones were recognized from the Visean to Serpukhovian, which can be used for stratigraphic correlation (Hounslow et al., 2004).

The Carboniferous is overall the apex of the late Paleozoic ice age. The integrated studies on paleoenvironments and biotic evolution have become major subjects worldwide. China has varied Carboniferous sedimentary facies, including mid- to high-latitude Gondwanan successions and low-latitude Paleo-Tethys successions. Future studies should focus on Carboniferous paleoenvironments and paleoclimate, based on variable proxies such as strontium and oxygen isotopes and stomatal index of fossil plants. Stratigraphic correlation between shallow- and deep-water successions, as well as high-resolution astronomical cyclostratigraphy, need to be further stressed to promote the research level and international status with respect to the Carboniferous of China.

Acknowledgements This work was supported by the Chinese Academy of Sciences (Grant Nos. XDB26000000, 18000000 and XDPB05), the National Natural Science Foundation of China (Grant No. 41290263), and the Ministry of Science and Technology of China (Grant No. 2013FY111000).

References

Alekseev A S, Goreva N V, Isakova T N, Makhlina M Kh. 2004. Biostratigraphy of the Carboniferous in the Moscow Syncline, Russia.

- News! Carb Stratigr, 22: 28–35
- Alekseev A S, Kononova L I, Nikishin A M. 1996. The Devonian and Carboniferous of the Moscow Syncline (Russian Platform): Stratigraphy and sea-level changes. *Tectonophysics*, 268: 149–168
- Aretz M, Chevalier E. 2007. After the collapse of stromatopod-coral reefs—the Famennian and Dinantian reefs of Belgium: Much more than Waulsortian mounds. In: Álvaro J J, Aretz M, Boulvain F, Munnecke A, Vachard D, Vennin E, eds. *Palaeozoic Reefs and Bioaccumulations: Climatic and Evolutionary Controls*. Geol Soc Spec Publ, 275: 163–188
- Aretz M, Poty E, Devuyt F X, Hance L, Hou H. 2012. Late Tournaisian Waulsortian-like carbonate mud banks from South China (Longdianshan Hill, central Guangxi): Preliminary investigations. *Geol J*, 47: 450–461
- Aretz M, Webb G E. 2007. Western European and eastern Australian Mississippian shallow-water reefs: a comparison. In: Wong T E, ed. *Proceedings of the XVth International Congress on Carboniferous and Permian Stratigraphy*. Utrecht, the Netherlands, 10–16 August 2003. Den Haag: Royal Netherlands Academy of Arts and Sciences. 433–442
- Barrick J E, Lambert L L, Heckel P H, Darwin R B. 2004. Pennsylvanian conodont zonation for Midcontinent North America. *Rev Espan Micropaleontol*, 36: 231–250
- Barrick J E, Lambert L L, Heckel P H, Rosscoe S J, Boardman D R. 2013. Midcontinent Pennsylvanian conodont zonation. *Stratigraphy*, 10: 55–72
- Barskov I S. 1984. Upper Carboniferous and Permian (Asselian) conodont zonation and zonal scale and problems of its perfection. In: Menner V V, Grigorieva A D, eds. *Upper Carboniferous of the USSR. Proceedings of the Interdepartmental Stratigraphic Committee of the USSR*, 13: 102–107
- Batt L S, Montañez I P, Isaacson P, Pope M C, Butts S H, Ablanaj J. 2007. Multi-carbonate component reconstruction of mid-carboniferous (Chesterian) seawater $\delta^{13}\text{C}$. *Palaeogeogr Palaeoclimatol Palaeoecol*, 256: 298–318
- Berner R A. 1990. Atmospheric carbon dioxide levels over Phanerozoic Time. *Science*, 249: 1382–1386
- Berner R A. 1997. The rise of plants and their effect on weathering and atmospheric CO_2 . *Science*, 276: 544–546
- Brand U, Tazawa J I, Sano H, Azmy K, Lee X. 2009. Is mid-late Paleozoic ocean-water chemistry coupled with epeiric seawater isotope records? *Geology*, 37: 823–826
- Bruckschen P, Bruhn F, Veizer J, Buhl D. 1995. isotopic evolution of Lower Carboniferous seawater: Dinantian of western Europe. *Sediment Geol*, 100: 63–81
- Bruckschen P, Oesmann S, Veizer J. 1999. Isotope stratigraphy of the European Carboniferous: Proxy signals for ocean chemistry, climate and tectonics. *Chem Geol*, 161: 127–163
- Buggisch W, Joachimski M M, Sevastopulo G, Morrow J R. 2008. Mississippian $\delta^{13}\text{C}_{\text{carb}}$ and conodont apatite $\delta^{18}\text{O}$ records — Their relation to the Late Palaeozoic Glaciation. *Palaeogeogr Palaeoclimatol Palaeoecol*, 268: 273–292
- Buggisch W, Wang X, Alekseev A S, Joachimski M M. 2011. Carboniferous-Permian carbon isotope stratigraphy of successions from China (Yangtze platform), USA (Kansas) and Russia (Moscow Basin and Urals). *Palaeogeogr Palaeoclimatol Palaeoecol*, 301: 18–38
- Caplan M L, Bustin R M. 1999. Devonian-Carboniferous Hangenberg mass extinction event, widespread organic-rich mudrock and anoxia: Causes and consequences. *Palaeogeogr Palaeoclimatol Palaeoecol*, 148: 187–207
- Chao Y T. 1927. Productidae of China (part 1). *Palaeontol Sin Ser B*, 5: 1–244
- Chao Y T. 1928. Productidae of China (part 2). *Palaeontol Sin Ser B*, 5: 1–100
- Chao Y T. 1929. Carboniferous and Permian spiriferids of China. *Palaeont Sin Ser B*, 11: 1–133
- Chen B, Joachimski M M, Wang X, Shen S, Qi Y, Qie W. 2016. Ice volume and paleoclimate history of the Late Paleozoic Ice Age from conodont apatite oxygen isotopes from Naqing (Guizhou, China). *Palaeogeogr Palaeoclimatol Palaeoecol*, 448: 151–161
- Chen J, Montañez I P, Qi Y, Shen S, Wang X. 2018. Strontium and carbon isotopic evidence for decoupling of $p\text{CO}_2$ from continental weathering at the apex of the late Paleozoic glaciation. *Geology*, 46: 395–398
- Chen J, Montañez I P, Qi Y, Wang X, Wang Q, Lin W. 2016. Coupled sedimentary and $\delta^{13}\text{C}$ records of late Mississippian platform-to-slope successions from South China: Insight into $\delta^{13}\text{C}$ chemostratigraphy. *Palaeogeogr Palaeoclimatol Palaeoecol*, 448: 162–178
- Chen S. 1934a. Fusulinidae of the Huanglung and Maping limestones, Kwangsi. *Mem Nat Res Ins Geol*, 14: 33–54
- Chen S. 1934b. Fusulinidae of South China, Part 1. *Palaeont Sin Ser B*, 4: 1–185
- Cohen K M, Finney S C, Gibbard P L, Fan J X. 2013. The ICS International Chronostratigraphic Chart. *Episodes*, 36: 199–204
- Collinson C, Rexroad C B, Thompson T L. 1971. Conodont Zonation of the North American Mississippian. *Geol Soc Am Mem*, 127: 358–394
- Danshin, B M. 1947. Geological Structure and Minerals of Moscow and its Environs (in Russian). Moscow: Moscow Society of Naturalist Press. 308
- Davydov V I, Crowley J L, Schmitz M D, Poletaev V I. 2010. High-precision U-Pb zircon age calibration of the global Carboniferous time scale and Milankovitch band cyclicity in the Donets Basin, eastern Ukraine. *Geochem Geophys Geosyst*, 11: Q0AA04–22
- Devuyt F-X, Hance L, Hou H F, Wu X H, Tian S G, Coen M, Sevastopulo G. 2003. A proposed global stratotype section and point for the base of the Visean Stage (Carboniferous): The Pengchong section, Guangxi, South China. *Episodes*, 26: 105–115
- Eros J M, Montañez I P, Osleger D A, Davydov V I, Nemyrovska T I, Poletaev V I, Zhykalyak M V. 2012. Sequence stratigraphy and onlap history of the Donets Basin, Ukraine: Insight into Carboniferous ice-house dynamics. *Palaeogeogr Palaeoclimatol Palaeoecol*, 313-314: 1–25
- Fan J S, Rigby J K. 1994. Upper carboniferous phylloid algal mounds in South Guizhou, China. *Brigham Young Univ Geol Stud*, 40: 17–24
- Fielding C R, Frank T D, Birgenheier L P, Rygel M C, Jones A T, Roberts J. 2008. Stratigraphic imprint of the Late Paleozoic Ice Age in eastern Australia: A record of alternating glacial and nonglacial climate regime. *J Geol Soc*, 165: 129–140
- Gong E P, Samankassou E, Guan C Q, Zhang Y L, Sun B L. 2007. Paleocology of Pennsylvanian phylloid algal buildups in south Guizhou, China. *Facies*, 54: 615–623
- Gong E P, Zhang Y L, Guan C Q. 2012. The Carboniferous reefs in China. *J Palaeogeogr*, 1: 27–42
- Goreva N, Alekseev A, Isakova T, Kossovaya O. 2009. Biostratigraphical analysis of the Moscovian-Kasimovian transition at the neostatotype of Kasimovian Stage (Afanasiovo section, Moscow Basin, Russia). *Palaeoworld*, 18: 102–113
- Goreva N V, Alekseev A S. 2010. Upper carboniferous conodont zones of Russia and their global correlation. *Stratigr Geol Correl*, 18: 593–606
- Grabau A W. 1936. Fauna of the Maping Limestone of Kwangsi and Kweichow. *Palaeont Sin Ser B*, 8: 1–441
- Grossman E L, Yancey T E, Jones T E, Bruckschen P, Chuvashov B, Mazzullo S J, Mii H. 2008. Glaciation, aridification, and carbon sequestration in the Permo-Carboniferous: The isotopic record from low latitudes. *Palaeogeogr Palaeoclimatol Palaeoecol*, 268: 222–233
- Hance L, Hou H F, Vachard D. 2011. Upper Famennian to Visean Foraminifers and Some Carbonate Microproblematica from South China—Hunan, Guangxi and Guizhou. Beijing: Geological Publishing House. 359
- Hance L, Poty E, Devuyt F X. 2006a. Tournaisian. In: Dejonghe L, ed. *Current status of chronostratigraphic units named from Belgium and adjacent areas*. *Geol Belg*, 9: 47–53
- Hance L, Poty E, Devuyt F X. 2006b. Visean. In: Dejonghe L, ed. *Current status of chronostratigraphic units named from Belgium and adjacent areas*. *Geol Belg*, 9: 55–62
- Heckel P H, Alekseev A S, Barrick J E, Boardman D R, Goreva N V, Isakova T N, Nemyrovska T I, Ueno K, Villa E, Work D M. 2008.

- Choice of conodont *Idiognathodus simulator* (*sensu stricto*) as the event marker for the base of the global Gzhelian Stage (Upper Pennsylvanian Series, Carboniferous System). *Episodes*, 31: 319–325
- Heckel P H. 2001. New proposal for series and stage subdivision of Carboniferous System. *Newsl Carb Stratigr*, 19: 12–14
- Heckel P H. 2008. Pennsylvanian cyclothems in Midcontinent North America as far-field effects of waxing and waning of Gondwana ice sheets. In: Fielding C R, Frank T D, Isbell J L, eds. *Resolving the Late Paleozoic Ice Age in Time and Space*. *Geol Soc Am Boulder Spec Publ*, 441: 275–289
- Henderson C M, Wardlaw B R, Vladimir I D, Schmitz M D, Schiappa T A, Tierney K E, Shen S Z. 2012. Proposal for base-Kungurian GSSP. *Permophiles*, 56: 8–21
- Hou H F, Wang Z J, Wu X H, Yang S P. 1982. The Carboniferous system of China. In: Chinese Academy of Geological Sciences, ed. *Stratigraphy in China (1): Introduction* (in Chinese with English abstract). Beijing: Geological Publishing House. 187–218
- Hou H F, Wu X H, Zhou H L, Hance L, Devuyt F X, Sevastopulo G. 2013. The GSSP for Visean stage (Mississippian Subsystem, Carboniferous System). In: Nanjing Institute of Geology and Palaeontology, Chinese Academy of Sciences, ed. *Global Standard Stratotype-sections and Points in China* (In Chinese). Hangzhou: Hangzhou University Press. 215–239
- Hou H F, Zhou H L, Liu J B. 2011. Microbial sediments occurring after the end-Devonian extinction event on the Hunan Platform (in Chinese with English abstract). *Acta Geol Sin*, 85: 145–156
- Hounslow M W, Davydov V I, Klootwijk C T, Turner P. 2004. Magnetostratigraphy of the Carboniferous: A review and future prospects. *Newsl Carb Stratigr* 22: 35–41
- Hu K Y. 2016. Early-Middle Pennsylvanian conodonts of South China and their global correlation. Doctoral Dissertation. Beijing: The University of Chinese Academy of Sciences. 1–289
- Hu K Y, Qi Y P, Wang Q L, Nemyrovska T I, Chen J T. 2017. Early Pennsylvanian conodonts from the Luokun section of Luodian, Guizhou, South China. *Palaeoworld*, 26: 64–82
- Hu K, Qi Y. 2017. The Moscovian (Pennsylvanian) conodont genus *Swadelina* from Luodian, southern Guizhou, South China. *Stratigraphy*, 14: 197–215
- Ivanov A P. 1926. Middle and Upper Carboniferous deposits of Moscow province (in Russian). *Otdel Geologicheskii*, 5: 133–180
- Jin Y G, Fan Y N, Wang X D, Wang R N. 2000. *Stratigraphical Lexicon of China, Carboniferous System* (in Chinese). Beijing: Geological Publishing House. 138
- Jin Y G. Additional brachiopods from the Kinling Formation of the Lower Yangtze District (in Chinese with English abstract). *Acta Palaeontol Sin*, 9: 272–290
- Kaiser S I, Aretz M, Becker R T. 2016. The global Hangenberg Crisis (Devonian-Carboniferous transition): Review of a first-order mass extinction. In: Becker R T, Königshof P, Brett C E, eds. *Devonian Climate, Sea Level and Evolutionary Events*. *Geol Soc Spec Publ*, 423: 387–437
- Korn D, Klug C. 2015. Paleozoic ammonoid biostratigraphy. In: Klug C, Korn D, de Baets K, Kruta I, Mapes R H, eds. *Ammonoid Paleobiology: From Macroevolution to Paleogeography*. Dordrecht: Springer. 299–328
- Kulagina E I, Pazukhin V N, Kotschetkova N M, Sinitsyna Z A, Kochetova N N. 2001. Stratotipicheskie opornye razrezy bashkirskogo yarusy karbona Yuzhnogo Urala. Ufa: Gilem. 138
- Kump L R, Arthur M A. 1997. Global chemical erosion during the Cenozoic: weatherability balances the budgets. In: Ruddiman W F, ed. *Tectonic Uplift and Climate Change*. New York: Plenum Press. 399–426
- Lane H R, Brenckle P L. 2005. Type Mississippian Subdivisions and Biostratigraphic Succession. In: Heckel P H, ed. *Stratigraphy and Biostratigraphy of the Mississippian Subsystem (Carboniferous System) in its type region, the Mississippi River Valley of Illinois, Missouri, and Iowa*. Champaign: Illinois State Geological Survey. 76–105
- Lee J S. 1927. *Fusuliniidae of North China*. *Palaeont Sin Sers B*, 4: 1–172
- Lees A, Miller J. 1985. Facies variations in Waulsortian buildups: Part 2. Mid-Dinantian buildups from Europe and North America. *Geol J*, 20: 159–180
- Li R F, Liu B P, Zhao C L. 1997. Correlation of Carboniferous depositional sequences on the Yangtze Plate with others on a global scale (in Chinese with English abstract). *Acta Sediment Sin*, 15: 23–28
- Li S J. 1987. Late Early Carboniferous to early Late Carboniferous brachiopods from Qixu, Nandan, Guangxi and their palaeoecological significance. In: Wang C Y, ed. *Carboniferous Boundaries in China*. Beijing: Science Press. 132–150
- Liang X L, Wang M Q. 1991. Carboniferous cephalopods of Xinjiang (in Chinese with English abstract). *Palaeontol Sin N Ser B*, 27: 1–171
- Lin J X, Li J X, Sun Q Y. 1990. Late Palaeozoic Foraminifera from South China (in Chinese). Beijing: Science Press. 297
- Liu Z H. 2002. On factors of Carboniferous reef developing in Hunan: A comparing study with Akiyoshi reef in Japan (in Chinese with English abstract). *Chin J Geol*, 37: 38–46
- McArthur J M, Howarth R J, Shields G A. 2012. *Strontium Isotope Stratigraphy*. In: Gradstein F, Ogg J, Schmitz M, Ogg G, eds. *The Geologic Time Scale 2012*. London: Elsevier. 127–144
- Mii H, Grossman E L, Yancey T E. 1999. Carboniferous isotope stratigraphies of North America: Implications for Carboniferous paleoceanography and Mississippian glaciation. *Geological Soc Am Bull*, 111: 960–973
- Montañez I P, Poulsen C J. 2013. The Late Paleozoic Ice Age: An Evolving Paradigm. *Annu Rev Earth Planet Sci*, 41: 629–656
- Munier C, Lapparent A. 1893. Note sur la nomenclature des terrains sédimentaires. *Bulletin de la Société géologique de France*, 3^{ès}, 21: 438–488
- Myrow P M, Ramezani J, Hanson A E, Bowring S, Racki G, Rakociński M. 2014. High-precision U-Pb age and duration of the latest Devonian (Famennian) Hangenberg event, and its implications. *Terra Nova*, 26: 222–229
- Nemyrovska T I. 1999. Bashkirian conodonts of the Donets Basin, Ukraine. *Sci Geol*, 119: 1–115
- Nemyrovska T I. 2011. Preliminary Moscovian conodont scale of the Donets Basin, Ukraine. *Newsl Carb Stratigr*, 29: 56–61
- Nemyrovska T I. 2017. Late Mississippian-Middle Pennsylvanian conodont zonation of Ukraine. *Stratigraphy*, 14: 299–318
- Nikitin S N. 1890. The Carboniferous of the Moscow Basin and artesian water in the region of the Moscow Basin (in French). *Trans Geol Comm*, 5: 139–182
- Poletaev V I, Brazhnikova N E, Vasilyuk N P, Vdovenko M V. 1990. Local zones and major Lower Carboniferous biostratigraphic boundaries of the Donets Basin (Donbass), Ukraine, U.S.S.R. *Courier Forsch Senckenberg*, 130: 47–59
- Popp B N, Anderson T F, Sandberg P A. 1986. Brachiopods as indicators of original isotopic compositions in some Paleozoic limestones. *Geol Soc Am Bull*, 97: 1262–1269
- Poty E, Devuyt F X, Hance L. 2006. Upper Devonian and Mississippian foraminiferal and rugose coral zonations of Belgium and northern France: A tool for Eurasian correlations. *Geol Mag*, 143: 829–857
- Qi Y P, Hu K Y, Barrick J E, Wang Q L, Lin W. 2012. Discovery of the conodont lineage from *Idiognathodus swadei* to *I. turbatus* in South China and its implications (in Chinese with English abstract). *J Stratigr*, 36: 551–557
- Qi Y P, Lambert L L, Nemyrovska T I, Wang X D, Hu K Y, Wang Q L. 2016. Late Bashkirian and early Moscovian conodonts from the Naqing section, Luodian, Guizhou, South China. *Palaeoworld*, 25: 170–187
- Qi Y, Nemyrovska T I, Wang X, Chen J, Wang Z, Lane H R, Richards B C, Hu K, Wang Q. 2014. Late Visean-early Serpukhovian conodont succession at the Naqing (Nashui) section in Guizhou, South China. *Geol Mag*, 151: 254–268
- Qie W K, Zhang X H, Du Y S, Zhang Y. 2011. Lower Carboniferous carbon isotope stratigraphy in South China: Implications for the Late Paleozoic glaciation. *Sci China Earth Sci*, 54: 84–92
- Ramsbottom W H C. 1984. The founding of the Carboniferous System. In: Gordon M Jr, ed. *Official Reports. Compte Rendu IX Congrès Inter-*

- national du Stratigraphieet Géologie du Carbonifère, Washington & Champaign-Urbana 1979, 1: 109–112
- Richards B C. 2013. Current status of the International Carboniferous timescale. In: Lucas S G, ed. *The Carboniferous-Permian Transition*. New Mexico Mus Nat Hist Sci Bull, 60: 348–353
- Ross C A, Ross J R P. 1987. Late Paleozoic sea levels and depositional sequences. In: Ross C A, Haman D, eds. *Timing and Depositional History of Eustatic Sequences: Constraints on Seismic Stratigraphy*. Cushman Found Foraminiferal Res Spec Publ, 24: 137–149
- Ross C A, Ross J R P. 1988. Late Paleozoic transgressive-regressive deposition. In: Wilgus C K, Hastings B S, Kendall C G S C, eds. *Sea-level changes: An integrated approach*. Society of Economic Paleontologists and Mineralogists Special Publication, 227–247
- Rosscoe S J, Barrick J E. 2013. North American species of the conodont genus *Idiognathodus* from the Moscovian-Kasimovian boundary composite sequence and correlation of the Moscovian-Kasimovian Stage boundary. In: Lucas S G, Dimichele W A, Barrick J E, Schneider J W, Spielmann J A, eds. *The Carboniferous-Permian Transition*. New Mexico Mus Nat Hist Sci Bull, 60: 354–371
- Ruan Y P. 1981a. Devonian and earliest Carboniferous ammonoids from Guangxi and Guizhou (in Chinese with English abstract). *Mem Nanjing Ins Geol Palaeont Acad Sin*, 15: 1–152
- Ruan Y P. 1981b. Carboniferous ammonoid faunas from Qixu in Nandan of Guangxi (in Chinese with English abstract). *Mem Nanjing Ins Geol Palaeont Acad Sin*, 15: 152–232
- Ruan Y P, Zhou Z R. 1987. Carboniferous cephalopods in Ningxia Hui Autonomous Region. In: Ningxia Bureau of Geology and Mineralogy and Nanjing Institute of Geology and Palaeontology, ed. *Namurian Strata and Fossils of Ningxia, China* (in Chinese with English abstract). Nanjing: Nanjing University Press, 55–177
- Rui L, Wang Z H, Zhang L X. 1987. Luosuan Stage—A new chronostratigraphic unit for the lowermost Upper Carboniferous (in Chinese). *J Stratigr*, 11: 103–115
- Rygel M C, Fielding C R, Frank T D, Birgenheier L P. 2008. The magnitude of Late Paleozoic glacioeustatic fluctuations: A synthesis. *J Sediment Res*, 78: 500–511
- Saltzman M R. 2002. Carbon and oxygen isotope stratigraphy of the Lower Mississippian (Kinderhookian-lower Osagean), western United States: Implications for seawater chemistry and glaciation. *Geol Soc Am Bull*, 114: 96–108
- Saltzman M R. 2003. The Late Paleozoic Ice Age: Oceanic gateway or $p\text{CO}_2$? *Geology*, 31: 151–154
- Saltzman M R, Gonzalez L A, Lohmann K C. 2000. Earliest Carboniferous cooling step triggered by the Antler orogeny? *Geology*, 28: 347–350
- Saltzman M, Groessens E, Zhuravlev A. 2004. Carbon cycle models based on extreme changes in $\delta^{13}\text{C}$: An example from the lower Mississippian. *Palaeogeogr Palaeoclimatol Palaeoecol*, 213: 359–377
- Sandberg C A, Ziegler W, Leuteritz K, Brill S M. 1978. Phylogeny, speciation, and zonation of *Siphonodella* (Conodonta, Upper Devonian and Lower Carboniferous). *Newsl Stratigr*, 7: 102–120
- Schmidt H. 1925. Die carbonischen Goniatiten Deutschlands. *Jahrb Preuss Geol Landesanst*, 45: 489–609
- Semikhatova S V. 1934. Moscovian deposits of Lower and Middle Volga area and position of the Moscovian Stage in general Carboniferous scale of the US (in Russian). *Problems Soviet Geol*, 3/8: 73–92
- Sheng H B. 1983. The ammonoids of late Lower Carboniferous from Yongzhu Village, Xainza District in North Xizang (in Chinese with English abstract). *Contrib Geol Qinghai-Xizang Plateau*, 8: 41–68
- Sheng Q Y. 2016. Mississippian foraminifers from South China. Doctoral Dissertation. Beijing: The University of Chinese Academy of Sciences, 1–285
- Sheng Q, Wang X, Brenckle P, Huber B T. 2018. Serpukhovian (Mississippian) foraminiferal zones from the Fenghuangshan section, Anhui Province, South China: Implications for biostratigraphic correlations. *Geol J*, 53: 45–57
- Shi Y K, Yang X L, Liu J R. 2012. Early Carboniferous to Early Permian Fusulinids from Zongdi Section in Southern Guizhou (in Chinese with English summary). Beijing: Science Press, 271
- Tarling D H. 1991. Applications of Palaeomagnetism in the Carboniferous. *Compte Rendu XI Congres International de Stratigraphie et de Géologie du Carbonifère*, Beijing 1987, 1: 205–212
- Teodorovich G I. 1949. On the subdivision of Upper Carboniferous into stages (in Russian). *Doklady Akademii Nauk SSSR*, 67: 537–540
- Ting V K, Grabau A W. 1936. The Carboniferous of China and its bearing on the classification of the Mississippian and Pennsylvanian. *Rept 16th Internat Geol Congr 1933*, 1: 555–571
- Trapp E, Kaufmann B, Mezger K, Korn D, Weyer D. 2004. Numerical calibration of the Devonian-Carboniferous boundary: Two new U-Pb isotope dilution-thermal ionization mass spectrometry single-zircon ages from Hasselbachtal (Sauerland, Germany). *Geology*, 32: 857–860
- Ueno K, Hayakawa N, Nakazawa T, Wang Y, Wang X. 2013. Pennsylvanian-Early Permian cyclothem successions on the Yangtze Carbonate Platform, South China. *Geol Soc London Spec Publ*, 376: 235–267
- Ueno K, Task Group. 2014. Report of the task group to establish the Moscovian-Kasimovian and Kasimovian-Gzhelian boundaries. *Newsl Carb Stratigr*, 31: 36–40
- Ueno K, Task Group. 2017. Report of the task group to establish the Moscovian-Kasimovian and Kasimovian-Gzhelian boundaries. *Newsl Carb Stratigr*, 33: 18–20
- Veizer J, Ala D, Azmy K, Bruckschen P, Buhl D, Bruhn F, Carden G A F, Diener A, Ebneth S, Godderis Y, Jasper T, Korte C, Pawellek F, Podlaha O G, Strauss H. 1999. $^{87}\text{Sr}/^{86}\text{Sr}$, $\delta^{13}\text{C}$ and $\delta^{18}\text{O}$ evolution of Phanerozoic seawater. *Chem Geol*, 161: 59–88
- Villa E, Task Group. 2008. Progress report of the Task Group to establish the Moscovian-Kasimovian and Kasimovian-Gzhelian boundaries. *Newsl Carb Stratigr*, 26: 12–13
- Wagner R H, Winkler Prins C F. 1991. Major subdivisions of the Carboniferous System. *Compte Rendu XI Congres International de Stratigraphie et de Géologie du Carbonifère*, Beijing 1987, 1: 213–245
- Wagner R H, Winkler Prins C F. 2016. History and current status of the Pennsylvanian chronostratigraphic units: Problems of definition and interregional correlation. *Newsl Stratigr*, 49: 281–320
- Walliser O H. 1995. Global events in the Devonian and Carboniferous. In: Walliser O H, ed. *Global Events and Event Stratigraphy*. Berlin: Springer-Verlag, 225–250
- Wang K L. 1983. Early Carboniferous Foraminifera from Shaoyang area of Hunnan Province and their stratigraphic significance (in Chinese with English abstract). *Bull Nanjing Inst Geol Palaeont Acad Sin*, 6: 209–224
- Wang Q L. 2014. Conodonts from the Kasimovian-Gzhelian boundary intervals in South China. Master Thesis. Beijing: University of Chinese Academy of Sciences, 1–94
- Wang X D, Jin Y G. 2000. An outline of Carboniferous chronostratigraphy (in Chinese with English abstract). *J Stratigr*, 24: 90–98
- Wang X D, Jin Y G. 2003. Carboniferous Biostratigraphy of China. In: Zhang W T, Chen P J, Palmer A R, eds. *Biostratigraphy in China*. Beijing: Science Press, 281–330
- Wang X D, Jin Y G. 2005. Achievements in the establishment of the Carboniferous GSSPs (in Chinese with English abstract). *J Stratigr*, 29: 147–153
- Wang X, Qi Y, Lambert L, Wang Z, Wang Y, Hu K, Lin W, Chen B. 2011. A potential global standard stratotype-section and point of the Moscovian Stage (Carboniferous). *Acta Geol Sin*, 85: 366–372
- Wang X D, Qie W K, Sheng Q Y, Qi Y P, Wang Y, Liao Z T, Shen S Z, Ueno K. 2013. Carboniferous and Lower Permian sedimentological cycles and biotic events of South China. In: Gasiewicz A, Słowakiewicz M, eds. *Palaeozoic Climate Cycles: Their Evolutionary and Sedimentological Impact*. *Geol Soc Spec Publ*, 376: 33–46
- Wang X D, Wang X J, Zhang F, Zhang H. 2006. Diversity patterns of Carboniferous and Permian rugose corals in South China. *Geol J*, 41: 329–343
- Wang Z H. 1990. Conodont zonation of the Lower Carboniferous in South China and phylogeny of some important species. *Courier Forsch Senckenberg*, 130: 41–46

- Wang Z H, Qi Y P. 2003. Upper Carboniferous (Pennsylvanian) conodonts from South Guizhou of China. *Riv Ital Paleontol S*, 109: 379–397
- Wang Z H, Qi Y P, Wang X D. 2008. Stage boundaries of the Pennsylvanian in the Nashui Section, Luodian of Guizhou, South China (in Chinese with English abstract). *Acta Micropalaeont Sin*, 25: 205–214
- Wu W S, Zhao J M. 1989. Carboniferous and Early Permian Rugosa from Western Guizhou and Eastern Yunnan, SW. China (in Chinese with English summary). *Palaeontol Sin Ser B*, 21: 1–230
- Wu X H. 2008. Report on integrated study of the Chinese Dewuan (Mississippian). In: *The 3rd National Commission on Stratigraphy, ed. Reports on the Subdivision and Establishment of the Chinese Stages* (in Chinese). Beijing: Geological Publishing House. 255–286
- Yang F Q. 1978. The strata and Cephalopod fauna of the Lower and Middle Carboniferous in western Guizhou (in Chinese). *Prof Papers Stratigr Palaeont*, 5: 143–200
- Yang J Z, Sheng J Z, Wu W S, Lu L H. 1962. *Proceeding of The National Meeting on Stratigraphy, The Carboniferous in China* (in Chinese). Beijing: Science Press. 113
- Yang J Z, Wu W S, Zhang L X, Liang Z T, Ruan Y P. 1979. New perspectives on the Series level subdivision of Carboniferous (in Chinese). *Acta Stratigr Sin*, 3: 188–192
- Yao L, Qie W, Luo G, Liu J, Algeo T J, Bai X, Yang B, Wang X. 2015. The TICE event: Perturbation of carbon-nitrogen cycles during the mid-Tournaisian (Early Carboniferous) greenhouse-icehouse transition. *Chem Geol*, 401: 1–14
- Yao L, Aretz M, Chen J, Webb G E, Wang X. 2016. Global microbial carbonate proliferation after the end-Devonian mass extinction: Mainly controlled by demise of skeletal bioconstructors. *Sci Rep*, 6: 39694
- Yao L, Wang X D. 2016. Distribution and evolution of Carboniferous reefs in South China. *Palaeoworld*, 25: 362–376
- Yin T H. 1932. *Gastropoda of Penchi and Taiyuan Series*. *Palaeontol Sin Ser B*, 11: 1–53
- Yin T H. 1933. *Cephalopoda of Penchi and Taiyuan Series of North China*. *Palaeontol Sin Ser B*, 11: 1–46
- Yu C C. 1931. The correlation of the Fengning System, the Chinese Lower Carboniferous, as based on coral zones. *Geol Soc China Bull*, 10: 1–30
- Yu C C. 1933. Lower Carboniferous corals of China. *Palaeontol Sin Ser B*, 12: 1–211
- Yu C M. 1988. Devonian-Carboniferous boundary in Nanbiancun, Guilin, China — Aspects and Records. Beijing: Science Press. 379
- Zhang L X. 1987. *Carboniferous Stratigraphy in China*. Beijing: Science Press. 160
- Zhang L X, Zhou J P, Sheng J Z. 2010. Upper Carboniferous and Lower Permian Fusulinids from Western Guizhou (in Chinese with English summary). *Palaeontol Sin Ser B*, 34: 1–296
- Zhang Z Q. 1988. The Carboniferous System in China. *Newsl Stratigr*, 18: 51–73
- Zhang Z H, Wang Z H, Li C Q. 1988. A Suggestion for Classification of Permian in South Guizhou (in Chinese with English summary). Guiyang: Guizhou People's Publishing House. 113
- Zong P, Becker R T, Ma X. 2015. Upper Devonian (Famennian) and Lower Carboniferous (Tournaisian) ammonoids from western Junggar, Xinjiang, northwestern China—Stratigraphy, taxonomy and palaeobiogeography. *Palaeobio Palaeoenv*, 95: 159–202

(Responsible editor: Shuzhong SHEN)